Surface Waves on an Anisotropic Plasma Sheath

S. R. SESHADRI, SENIOR MEMBER, IEEE, AND W. F. PICKARD

Summary—**A treatment of the excitation of unidirectional plane surface waves on a perfectly conducting screen covered with an anisotropic plasma sheath is given for the case in which the external magnetic field is oriented parallel to the screen but perpendicular to the direction of propagation. The dispersion relations for the surface waves and their dependence on the strength of the external magnetic field and the sheath thickness, are discussed. For sufficiently small sheath thickness, backward surface waves are found to exist. The powers carried by the surface waves and the space waves are evaluated, and the efficiency of excitation of the surface waves are determined as a function of sheath thickness for a typical set of parameters. The power carried by the forward and backward surface waves are compared for two cases in which, in a given direction, either one or both of these exist.**

I. Introduction

THE EFFECT of a grounded dielectric slab on the radiation pattern of an electromagnetic source has been studied by a number of investigators. A majority of these investigations pertain to the case of a slab of isotropic dielectric. A complete survey of the relevant literature may be found in the recent work of Oliner and Tamir [1]–[4] who have given a comprehensive treatment of the electromagnetic field of a source-excited, isotropic plasma slab. There have been relatively fewer investigations of the effect of a slab of anisotropic dielectric. Wait [5], [6] has treated the case of a thin plasma sheet in free space as well as in the vicinity of a ground screen. The radiation pattern of a line source of magnetic current embedded in a plasma slab has been investigated for the case of an external magnetic field, perpendicular to the line source by Shore and Meltz [7] and parallel to it by Hodara and Cohn [8]. Ishimaru [9] has given an elegant treatment of the effect of leaky waves on the radiation from a plasma sheath. With the exception of the work of Wait, who has treated only the case of a thin plasma sheet, all of the above investigations of the anisotropic slab problem have been restricted to the treatment of the radiation pattern only. A systematic investigation of the wave supporting properties of an anisotropic slab, similar to the one carried out by Oliner and Tamir for the isotropic case, is not available.

In this paper, a treatment of the radiation characteristics of a slot excited plasma slab is given for a particularly simple orientation of the external magnetic field. The slot is assumed to be infinitely long and infinitesimally narrow, with the external magnetic field oriented parallel to the slot. Particular emphasis is placed on the characteristics of the surface waves guided along the plasma sheath. This problem is the same as the one investigated by Hodara and Cohn [8] who have not, however, considered the excitation of the surface waves but have restricted their attention only to the radiation pattern.

The dispersion relations for the surface waves and their dependence on the strength of the external magnetic field and the sheath thickness, are examined in detail. For sufficiently small sheath thickness, backward surface waves are excited. The surface waves propagating in the two directions have different characteristics. The reversal of the direction of the external magnetic field reverses the direction of propagation of the surface waves. The powers carried by the surface waves and space waves are evaluated and the efficiency of excitation of surface waves determined as a function of the sheath thickness.

The power carried by the forward and the backward surface waves are compared for two cases in which either one or both of them travel in a given direction. For appropriate parameter values, only the backward surface wave may exist in a particular direction, enabling the possibility of its detection experimentally.

A comparison of the surface wave dispersion obtained in this case, with those for a perfectly conducting screen covered with a semi-infinite layer of plasma and for a plane interface between a semi-infinite free space and a semi-infinite gyrotropic plasma, is made for the low frequency limit. This enables the assessment of the importance of the role played by the two interfaces, the ground screen and the vacuum-plasma interface, in guiding the surface waves. There are three low-frequency surface waves, one of which may be identified as the unidirectional surface wave guided by the conducting plane and the other two, as the surface waves guided by the vacuum-plasma interface.

II. Formulation of the Problem

Consider a perfectly conducting screen of infinite extent, located in the xy-plane, where x, y, and z form a right-handed rectangular coordinate system (Fig. 1). The region $-\infty < x < \infty$, $-\infty < y < \infty$, and $0 < z < d$ is filled with uniform plasma, and the rest of the half-space $z > 0$ is vacuum. At $x = 0$, on the screen, there is a slot which is infinitely long in the y-direction, infinitesimally narrow in the x-direction and uniformly excited with an electric field in the x-direction. The source may therefore be represented by

$$E_x(x, 0) = E_{x0}\delta(x). \tag{1}$$

Manuscript received March 17, 1964; revised June 17, 1964. This research was supported, for the most part, by the National Science Foundation by Grants NSF-G9721 and NSF-G21869.

The authors are with the Gordon McKay Laboratory, Harvard University, Cambridge, Mass.

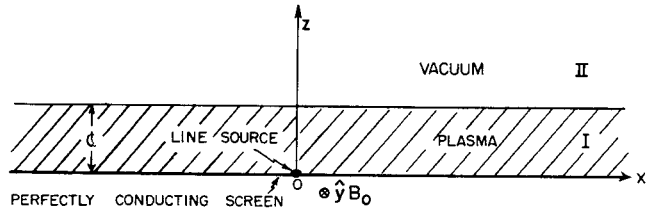

Fig. 1—Geometry of the problem.

A uniform static magnetic field B_0 is impressed in the y-direction throughout the plasma.

The source (1) may be shown [10], [11] to excite only the E mode which consists of a single component of the magnetic field H_y, specified by the following wave equations:

Region I

$$\left[\frac{\partial^2}{\partial x^2}+\frac{\partial^2}{\partial z^2}+k^2\right]H_y(x, z) = 0 \quad 0 < z \leq d \tag{2}$$

Region II

$$\left[\frac{\partial^2}{\partial x^2}+\frac{\partial^2}{\partial z^2}+k_0^2\right]H_y(x, z) = 0 \quad d \leq z \leq \infty \tag{3}$$

where,

$$k^2 = \omega^2\mu_0\epsilon_0\frac{\epsilon}{\epsilon_1} = k_0^2\frac{(\epsilon_1^2-\epsilon_2^2)}{\epsilon_1} = k_0^2\frac{\epsilon}{\epsilon_1} \tag{4a}$$

$$\epsilon_1 = \frac{\Omega^2-R^2-1}{\Omega^2-R^2}, \quad \epsilon_2 = \frac{R}{\Omega(\Omega^2-R^2)}, \quad \Omega = \frac{\omega}{\omega_p},$$

$$R = \frac{\omega_c}{\omega_p}, \tag{4b}$$

and u_0, ϵ_0, ω_p, and ω_c are, respectively, the permeability and dielectric constant pertaining to vacuum and the plasma and the gyromagnetic frequency of the electrons. The nonvanishing components of the electric field $E_x(x, z)$ and $E_z(x, z)$ are obtained with the help of the following relations:

Region I

$$E_x(x, z) = \left(\frac{-i\epsilon_1}{\omega\epsilon_0\epsilon}\frac{\partial}{\partial z}-\frac{\epsilon_2}{\omega\epsilon_0\epsilon}\frac{\partial}{\partial x}\right)H_y(x, z) \tag{5a}$$

$$E_z(x, z) = \left(\frac{i\epsilon_1}{\omega\epsilon_0\epsilon}\frac{\partial}{\partial x}-\frac{\epsilon_2}{\omega\epsilon_0\epsilon}\frac{\partial}{\partial z}\right)H_y(x, z)$$

Region II

$$E_x(x, z) = \frac{-i}{\omega\epsilon_0}\frac{\partial}{\partial z}H_y(x, z),$$

$$E_z(x, z) = \frac{i}{\omega\epsilon_0}\frac{\partial}{\partial x}H_y(x, z). \tag{5b}$$

Note that all the field components are independent of y, and the harmonic time dependence $e^{-i\omega t}$ is implied for all of them.

In addition to the radiation condition at $z=\infty$ and the boundary condition (1) for $z=0$, the following boundary conditions must be satisfied at the vacuum-plasma interface:

$$H_y(x, d^-) = H_y(x, d^+); \quad E_x(x, d^-) = E_x(x, d^-). \tag{6}$$

The solutions of (2) and (3) together with (1) and (6) may be shown to yield the following integral expressions for $H_y(x, z)$:

$$H_y(x, z) = \frac{1}{2\pi}\int_{-\infty}^{\infty}\frac{\omega\epsilon_0\epsilon E_{x0}}{2\Delta(\zeta)}\left[(\epsilon_1\xi+\epsilon\xi_0+i\epsilon_2\zeta)e^{i\xi(z-d)}\right.$$
$$\left.+(\epsilon_1\xi-\epsilon\xi_0-i\epsilon_2\zeta)e^{-i\xi(z-d)}\right]e^{i\zeta x}d\zeta$$
$$\text{for } 0 < z < d \tag{7a}$$

$$H_y(x, z) = \frac{1}{2\pi}\int_{-\infty}^{\infty}\frac{\omega\epsilon_0\epsilon E_{x0}\epsilon_1\xi}{\Delta(\zeta)}e^{i\xi_0(z-d)+i\zeta x}d\zeta$$
$$\text{for } d < z < \infty \tag{7b}$$

where

$$\Delta(\zeta) = \epsilon\epsilon_1\xi\xi_0\cos\xi d - i\left\{k^2\epsilon_1^2-\epsilon\zeta^2-i\epsilon_2\epsilon\zeta\xi_0\right\}\sin\xi d \tag{8}$$

and

$$\xi = \begin{cases} +\sqrt{k^2-\zeta^2} & \text{for } k > \zeta \\ +i\sqrt{\zeta^2-k^2} & \text{for } k < \zeta \end{cases}$$

$$\xi = \begin{cases} +\sqrt{k_0^2-\zeta^2} & \text{for } k_0 > \zeta \\ +i\sqrt{\zeta^2-k_0^2} & \text{for } k_0 < \zeta. \end{cases} \tag{9}$$

III. Singularities of the Integrand

It is easily seen that the integrands in (7a, b) are even functions of ξ and the branch points occur on the real axis only for $\zeta = \pm k_0$. The poles of the integrands in (7a, b) obviously occur at the zeros of $\Delta(\zeta)$. The necessary condition for $H_y(x, z)$ to have surface wave contributions is that $\Delta(\zeta)$ should have real zeros, k_s. Consequently, the real roots k_s of

$$\Delta(\zeta) = 0 \tag{10}$$

will be considered first. Let

$$\xi = k_0\alpha \quad \xi_0 = k_0\alpha_0 \quad k_s = k_0\zeta_s \quad k_0d = \beta, \tag{11}$$

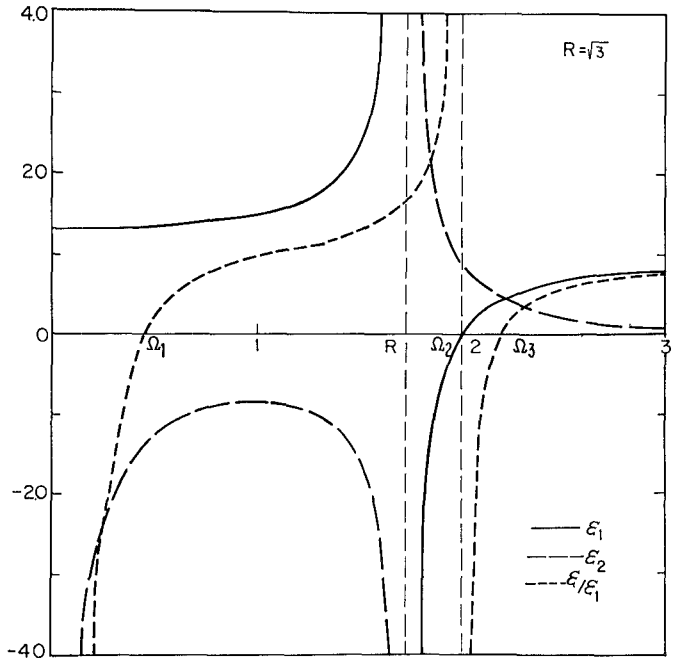

Fig. 2—ϵ_1, ϵ_2, and ϵ/ϵ_1 as a function of Ω.

where it might be noted that ζ_s is nondimensional. In view of (9) and (11), it follows that

$$\alpha = \begin{cases} +\sqrt{\dfrac{\epsilon}{\epsilon_1} - \zeta_s^2} \\ +i\sqrt{\zeta_s^2 - \dfrac{\epsilon}{\epsilon_1}} \end{cases} \quad \text{for} \quad \frac{\epsilon}{\epsilon_1} \gtrless \zeta_s^2;$$

$$\alpha_0 = \begin{cases} +\sqrt{1-\zeta_s^2} \\ +i\sqrt{\zeta_s^2 - 1} \end{cases} \quad \text{for} \quad 1 \gtrless \zeta_s^2. \tag{12}$$

Together with (8) and (11), (10) may be recast in the form

$$\tan \beta\alpha = \frac{-i\alpha\alpha_0}{1 - \dfrac{\zeta_s^2}{\epsilon_1} - \dfrac{i\epsilon_2}{\epsilon_1}\zeta_s\alpha_0}. \tag{13}$$

The right-hand side of (13) is not an even function of ζ_s with the result that the real roots ζ_s of (13) are not symmetrical about $\zeta_s = 0$. It may be shown that ϵ_2 changes sign when the direction of the external magnetic field is reversed. Also when ϵ_2 and ζ_s both change sign, (13) is unchanged. Therefore, the reversal of the direction of the external magnetic field is seen to result in the interchange of the positive and negative roots of (13).

It is useful to examine first, the behavior of ϵ_1, ϵ_2, and ϵ/ϵ_1 as a function of Ω. With the help of (4b), the following results may be easily established:

$$\infty > \epsilon_1 > 1 \quad \text{for} \quad 0 < \Omega < R \tag{14a}$$

$$1 > \epsilon_1 > 0 \quad \text{for} \quad \Omega_2 < \Omega < \infty \tag{14b}$$

$$-\infty < \epsilon_1 < 0 \quad \text{for} \quad R < \Omega < \Omega_2 \tag{14c}$$

$$\epsilon_2 \lessgtr 0 \quad \text{for} \quad \Omega \lessgtr R \tag{14d}$$

$$\epsilon_2 = -\infty \quad \text{for} \quad \Omega = 0 \tag{14e}$$

$$\epsilon_2 < 1 \quad \text{for} \quad \Omega > \Omega_2 \tag{14f}$$

$$0 < \frac{\epsilon}{\epsilon_1} \leq 1 \quad \text{for} \quad \Omega_1 < \Omega < 1 \quad \text{and} \quad \Omega_3 < \Omega < \infty \tag{14g}$$

$$1 < \frac{\epsilon}{\epsilon_1} \leq \infty \quad \text{for} \quad 1 < \Omega < \Omega_2 \tag{14h}$$

$$-\infty < \frac{\epsilon}{\epsilon_1} < 1 \quad \text{for} \quad 0 < \Omega < \Omega_1 \quad \text{and} \quad \Omega_2 < \Omega < \Omega_3 \tag{14i}$$

$$\frac{\epsilon}{\epsilon_1} = -\infty \quad \text{for} \quad \Omega = 0 \tag{14j}$$

where

$$\Omega_{1,3} = \frac{\mp R + \sqrt{R^2+4}}{2} \qquad \Omega_2 = \sqrt{1+R^2}. \tag{15}$$

The behavior of ϵ_1, ϵ_2, and ϵ/ϵ_1 as a function of Ω, is depicted in Fig. 2 for a particular value of R.

In determining the real roots of (13), it is advantageous to distinguish the following four cases:

$$\text{case 1: } \zeta_s^2 \le 1 \quad \zeta_s^2 \le \frac{\epsilon}{\epsilon_1} \quad \alpha = |\alpha| \quad \alpha_0 = |\alpha_0|$$

$$\text{case 2: } \zeta_s^2 \le 1 \quad \zeta_s^2 \ge \frac{\epsilon}{\epsilon_1} \quad \alpha = i|\alpha| \quad \alpha_0 = |\alpha_0|$$

$$\text{case 3: } \zeta_s^2 \ge 1 \quad \zeta_s^2 \le \frac{\epsilon}{\epsilon_1} \quad \alpha = |\alpha| \quad \alpha_0 = i|\alpha_0|$$

$$\text{case 4: } \zeta_s^2 \ge 1 \quad \zeta_s^2 \ge \frac{\epsilon}{\epsilon_1} \quad \alpha = i|\alpha| \quad \alpha_0 = i|\alpha_0|. \tag{16}$$

For the cases 1 and 2, (13) which specifies ζ_s becomes

$$\begin{matrix}\text{case 1:} \quad \tan\beta|\alpha| \\ \text{case 2:} \quad \tanh\beta|\alpha|\end{matrix} = \frac{-i|\alpha|\,|\alpha_0|}{1 - \dfrac{\zeta_s^2}{\epsilon_1} - \dfrac{i\epsilon_2}{\epsilon_1}\zeta_s|\alpha_0|}. \tag{17}$$

For (17) to hold, the following equalities must be simultaneously fulfilled:

$$\text{case 1:} \quad \begin{matrix}\left(1 - \dfrac{\zeta_s^2}{\epsilon_1}\right)\tan\beta = 0 \\ \left(|\alpha|\,|\alpha_0| - \dfrac{\epsilon_2}{\epsilon_1}\zeta_s|\alpha_0|\tan\beta\right) = 0\end{matrix} \tag{18a, b}$$

case 2: same as (18) with tan replaced by tanh. (19a, b)

Since $\zeta_s^2 \le (\epsilon/\epsilon_1)$, it follows that $1-(\zeta_s^2/\epsilon_1) \ge (\epsilon_2^2/\epsilon_1^2)$ and therefore, (18a, b) and (19a, b) are satisfied only for $\alpha = 0$. Also the numerators of the integrands in (7a, b) are seen to vanish for $|\alpha| = 0$ and hence, $|\alpha| = 0$ is not a pole. Therefore, the integrands of (7a, b) do not have real poles in the first two cases. Note that both the cases 1 and 2 correspond to a fast wave, and it is to be expected that there should be no fast wave with real propagation constant for an open structure such as the one considered in this paper.

For the cases 3 and 4, (13) becomes

$$|\alpha|\,|\alpha_0| \Big/ \left(1 - \frac{\zeta_s^2}{\epsilon_1} + \frac{\epsilon_2}{\epsilon_1}\zeta_s|\alpha_0|\right) = \begin{cases}\tan\beta|\alpha| & \text{for case 3} \quad (20)\\ \tanh\beta|\alpha| & \text{for case 4} \quad (21)\end{cases}$$

A real ζ_s which satisfies (20) and (21) can be found. In view of (14h), the conditions $\zeta_s^2 \ge 1$ and $\zeta_s^2 \le \epsilon/\epsilon_1$ can be simultaneously fulfilled only in the frequency range $1 < \Omega < \sqrt{1+R^2}$, but the conditions $\zeta_s^2 \ge 1$ and $\zeta_s^2 \ge \epsilon/\epsilon_1$ can be satisfied in the entire frequency range. Since ζ_s is real and $\zeta_s^2 \ge 1$, it follows from (7a, b) that the fields in the vacuum region for the cases 3 and 4 decay exponentially transverse to the slab and propagate without attenuation along the slab. For the case 3 (case 4), the contribution to $H_y(x, z)$ given in (7a) arising from a pole specified by (20) [(21)] is such that the fields inside the plasma slab have a functional dependence on z which is of the trigonometric (hyperbolic) type, and the corresponding surface wave will be designated for convenience as Type 1 (Type 2). Evidently, Type 1 surface wave exists only in the frequency range $1 < \Omega < \sqrt{1+R^2}$.

For $\sqrt{1+R^2} < \Omega < \infty$, if there is any surface wave at all, it should obviously be of the type 2 and, therefore, should arise from the real roots of (21). It will be shown now that (21) has no real roots for $\sqrt{1+R^2} < \Omega < \infty$. Let the denominator of the left side of (21) be denoted by $D(\zeta_s)$. For $\sqrt{1+R^2} < \Omega < \infty$, it follows from (14b and 6) that $0 \le \epsilon_1 < 1$ and $0 \le |\epsilon_2| < 1$. If the orientation of the external magnetic field is such that $\epsilon_2\zeta_s < 0$, then $D(\zeta_s) < 0$ over the entire range of ζ_s. Even if $\epsilon_2\zeta_s > 0$, it can be shown that $D(\zeta_s) < 0$. Let $P(\zeta_s) = (|\epsilon_2|\zeta_s|\alpha_0|)/(\zeta_s^2 - \epsilon_1)$. It follows from the definition of $D(\zeta_s)$ and the fact that $\zeta_s \ge 1 > \epsilon_1$, that $D(\zeta_s) < 0$ provided $P(\zeta_s) < 1$. Obviously, at the end points of the range of ζ_s, namely 1 and ∞, $P(\zeta_s) < 1$. It can be easily shown that $P(\zeta_s)$ is a maximum when $\zeta_s = \sqrt{\epsilon_1/(2\epsilon_1 - 1)}$. Consequently for $0 < \epsilon_1 < \frac{1}{2}$, $P(\zeta_s)$ has no maximum in the range $1 < \zeta_s < \infty$. Hence, it follows that $P(\zeta_s) < 1$, as at the end points for the entire range of ζ_s. For $\frac{1}{2} < \epsilon_1 < 1$, $P(\zeta_s)$ has a maximum which is given by

$$P(\zeta_s)_{\max} = \frac{R}{2\Omega}\,\frac{1}{\sqrt{\Omega^2 - R^2 - 1}}. \tag{22}$$

For $\sqrt{1+R^2} < \Omega < \infty$, $P(\zeta_s)_{\max}$ and hence, $P(\zeta_s) < 1$. Therefore, $D(\zeta_s) < 0$ for the entire range of ζ_s. Since the right-hand side of (21) as well as the numerator of the left side of (21) is always positive for $1 < \zeta_s < \infty$, it follows that no real ζ_s can satisfy (21) for $\sqrt{1+R^2} < \Omega < \infty$ since the denominator of the left side of (21) is always negative. Hence, it follows that the Type 2 surface waves arising from the real roots of (21) exist only in the frequency range $0 < \Omega < \sqrt{1+R^2}$. Since the Type 1 surface waves exist only for $1 < \Omega < \sqrt{1+R^2}$, it is clear that the surface waves are restricted to the frequency range $0 < \Omega < \sqrt{1+R^2}$.

IV. Dispersion Curves for the Surface Waves

The real roots ζ_s of (20) and (21) were obtained numerically for three values of the parameter R which is proportional to the external magnetic field. Since the frequency ω and the wave number k_s of the surface wave are respectively proportional to Ω and $\Omega\zeta_s$, the dispersion diagram corresponds to a plot of Ω vs $\Omega\zeta_s$, and these plots are depicted in Figs. 3–5 (pages 534–535). In each case, the results are given for three values of the thickness parameter β, namely, $\beta = 10$, 1, and 0.1.

As was stated before, Type 1 surface waves exist only for $1 < \Omega < \sqrt{1+R^2}$. An examination of Figs. 3–5 shows that for $\Omega = 1$ there are no Type 1 surface waves. As Ω is increased beyond 1, the first Type 1 surface wave comes into existence at a particular value of Ω. When Ω

is still further increased, the wave number of the surface waves increases monotonically; other Type 1 surface waves appear abruptly and then continue with increasing Ω and $\Omega\zeta_s$. Theoretically, for $\Omega=\sqrt{1+R^2}$, there is an infinity of such waves. These surface waves have different characteristics depending on whether they propagate in the positive or the negative x-direction. The Type 1 surface waves are seen to have a low-frequency cutoff and are always forward waves in the sense that their phase and group velocities are of the same sign. In general, for a given Ω in the range $1<\Omega<\sqrt{1+R^2}$, an increase in the thickness β of the slab, results in an increase of the number of the surface wave poles. It is to be noted that the surface wave poles in the vicinity of $\Omega=\sqrt{1+R^2}$, have not been determined and are not included in Figs. 3–5.

For the Type 2 surface waves, it is seen that in general, there is only one dispersion curve for positive values of the wave number, but there are two for negative values of the wave number. For $R=0.1$, the second dispersion curve for the negative values of the wave number does not show up, but for $R=0.5$ and 2.0, both the dispersion curves are clearly seen. The Type 2 surface waves have no low frequency cutoff. For very large positive values of the surface wave number, the dispersion curve asymptotically reaches a particular value of Ω. The dispersion curve always finally approaches the asymptote from smaller values of Ω, but for very small β, it crosses the asymptote twice and then, as for larger values of β, it approaches the asymptote from smaller values of Ω. The result of such a dispersion is that for Ω slightly greater than the asymptotic value, there are two surface waves, with their phase fronts propagating in the positive x-direction, and one of them is a backward wave. Also, for values of Ω slightly less than the asymptotic value and for sufficiently small β, there are three surface waves of Type 2 of which one is a backward wave. The same general behavior is exhibited by the two dispersion curves which correspond to negative values of the wave number. It is seen that for $R=0.5$, the asymptotes for the two negative Type 2 surface waves coincide. Also, the numerical results indicate that, in general, only one of the dispersion curves, namely that which has a higher frequency cutoff, has a backward wave region.

Having obtained numerically that the dispersion curves for the Type 2 surface waves have asymptotes, it is an easy matter to obtain the equations for the asymptotes from (21). For $|\zeta_s|\to\infty$, with the help of (4b), (21) yields

$$1=\epsilon_1/(\epsilon_2\operatorname{sgn}\zeta_s-1)$$

$$=(\Omega^2-R^2-1)\Big/\left(\frac{R}{\Omega}\operatorname{sgn}\zeta_s-\Omega^2+R^2\right). \tag{23}$$

The positive value of Ω which satisfies (23) is given by

$$\Omega_{a1}=\frac{R+\sqrt{R^2+2}}{2} \qquad \zeta_s>0 \tag{24}$$

$$\Omega_{a2}=\frac{-R+\sqrt{R^2+2}}{2}; \quad \Omega_{a3}=R \quad \zeta_s<0. \tag{25a, b}$$

Since $|\zeta_s|=\infty$ corresponds on the dispersion curve to a Ω given by (24) and (25), it follows that $\Omega=\Omega_{a1}$ and $\Omega=\Omega_{a2}$, Ω_{a3} are the asymptotes for the dispersion curves corresponding to positive and negative wave numbers respectively. Note that $\Omega_{a2}=\Omega_{a3}$ for $R=0.5$. Hence, for $R=0.5$, there is only one asymptote on the negative side, and this is also obtained numerically as can be seen in Fig. 4. The other asymptotes in Figs. 3–5 are precisely those given by (24) and (25).

It was noticed that the dispersion curves for the Type 2 surface waves always approached the asymptote from smaller values of Ω. This can easily be proved with the help of (21). For very large ζ_s, (21) after some simplification, yields

$$\frac{1}{2\zeta_s^2}=\frac{\epsilon_2-1-\epsilon_1}{\epsilon_2-3\epsilon_1-\epsilon_1^2+\epsilon_2^2}. \tag{26}$$

As ζ_s becomes very large, the left side of (26) becomes a very small positive number. If the expressions given in (4b) for ϵ_1 and ϵ_2 are substituted on the right side of (26) and Ω is set equal to $\Omega_a+\delta$, where Ω_a is one of the asymptotes given by (24) and (25), and δ is an arbitrarily small real number, it is found after considerable manipulation that δ is negative; from this result, it is obvious that the dispersion curves approach the asymptotes from smaller values of Ω. As a consequence, it is clear that the dispersion curves, when they cross the asymptotes, do so an even number of times. Even though it is difficult to deduce theoretically from (21), the numerical results as depicted in Figs. 3–5 indicate that the asymptotes are crossed at most, twice.

In Fig. 6 (page 536), the dispersion curves for the Type 2 surface waves are shown for $R=0.5$ and for various values of the sheath thickness β. The dispersion curves for any value of $\beta>10$ do not differ appreciably from those for $\beta=10$. Note that for large values of β such as 10, the dispersion curves do not possess any backward wave regions. If β is reduced, the phase velocity of the surface wave is found to increase, and for $\beta=0.34$ in the present example, the dispersion curve corresponding to positive wave numbers develops a backward wave region. For this β (see inset to Fig. 6) at certain frequencies, there are three surface waves of which one is backward. Also, there is a high frequency cutoff Ω_c which is less than Ω_{a1}, and in the frequency range $\Omega_{a1}>\Omega>\Omega_c$, there is only one forward surface wave. Any further decrease in β results not only in speeding up of the forward and the slowing down of the backward surface waves but also in the increase of the cutoff frequency Ω_c. Finally for some value of β, namely $\beta=0.32$ approximately, in the present example, the high frequency

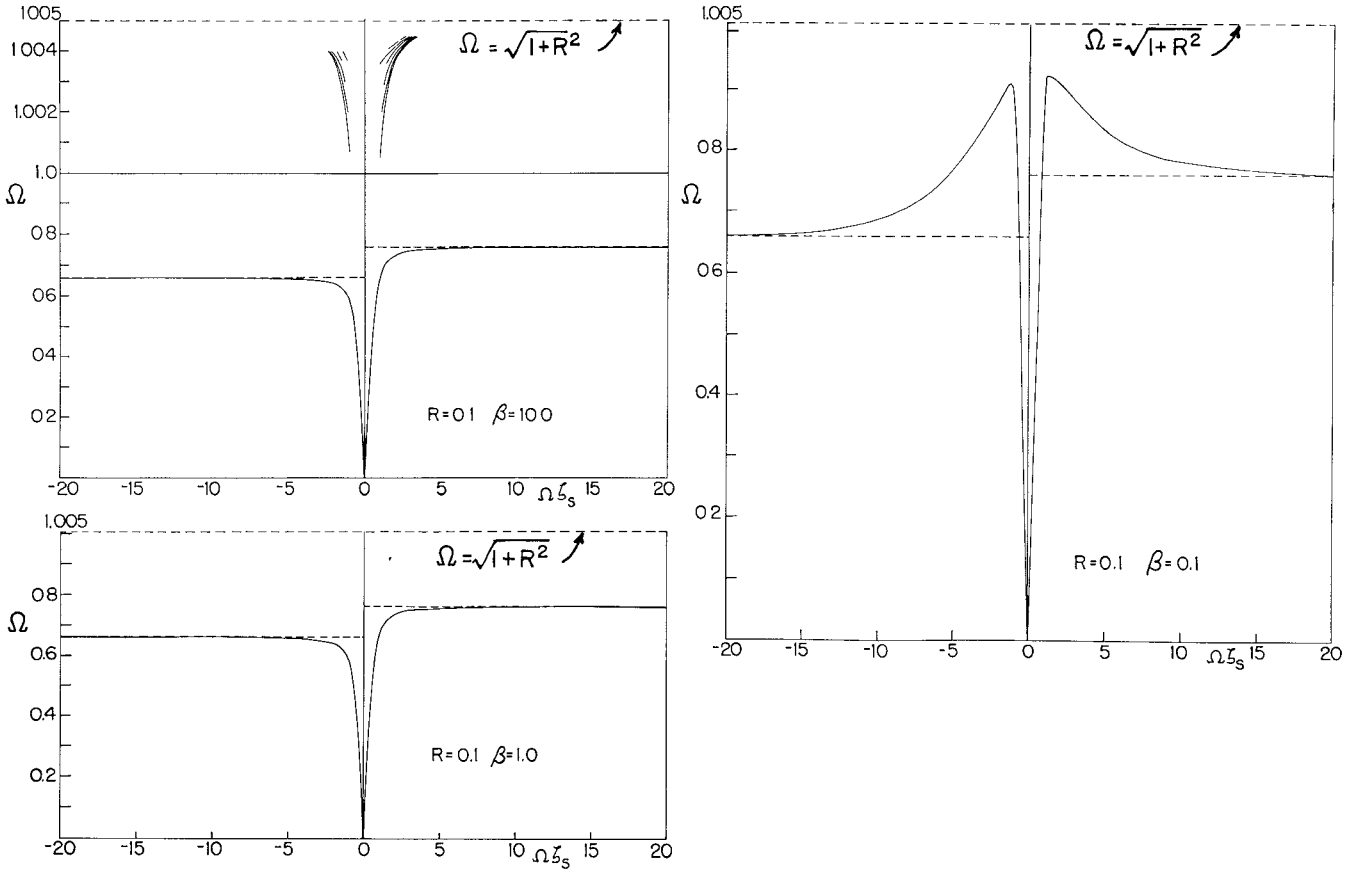

Fig. 3—Dispersion curves for the surface waves.

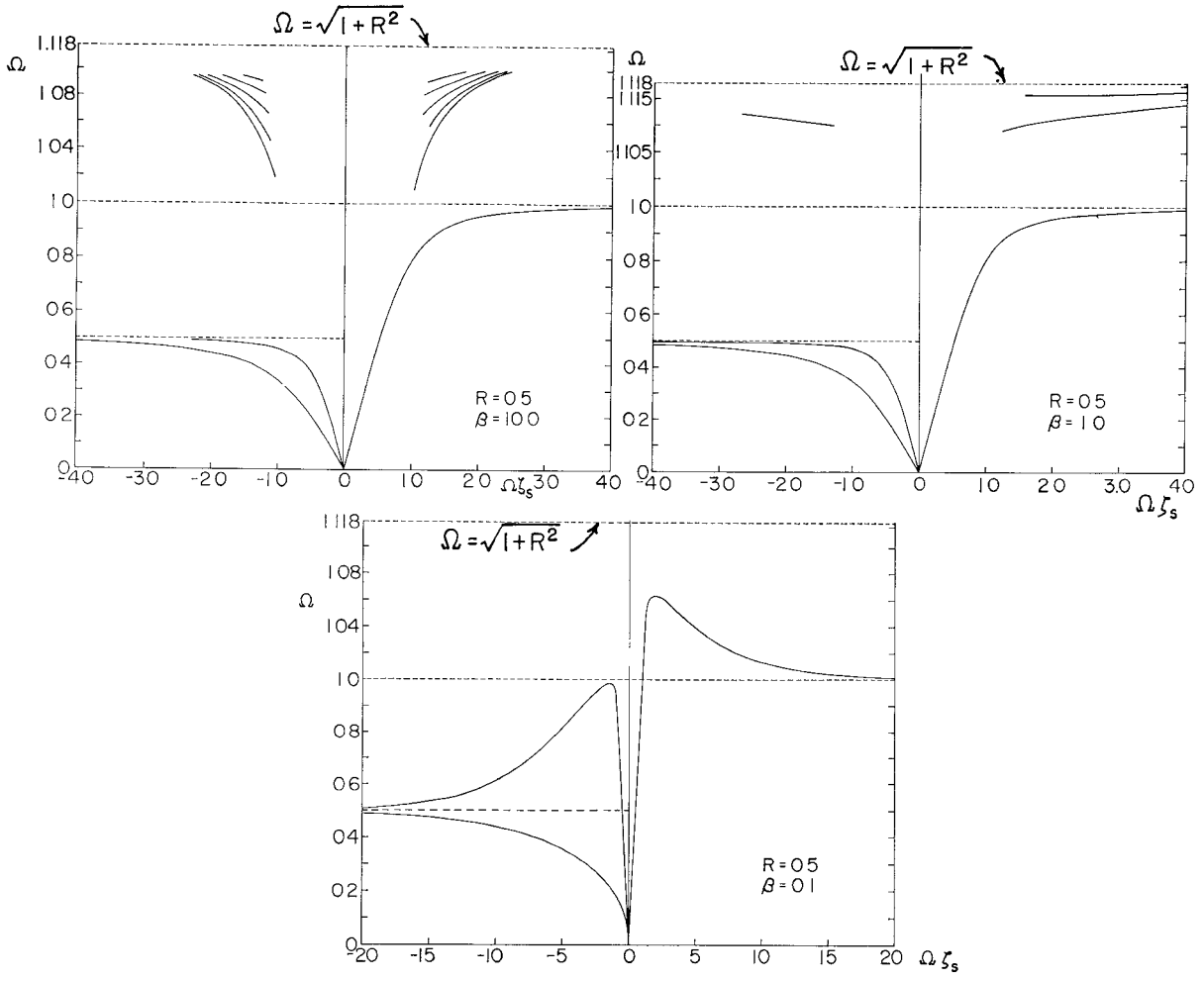

Fig. 4—Dispersion curves for the surface waves.

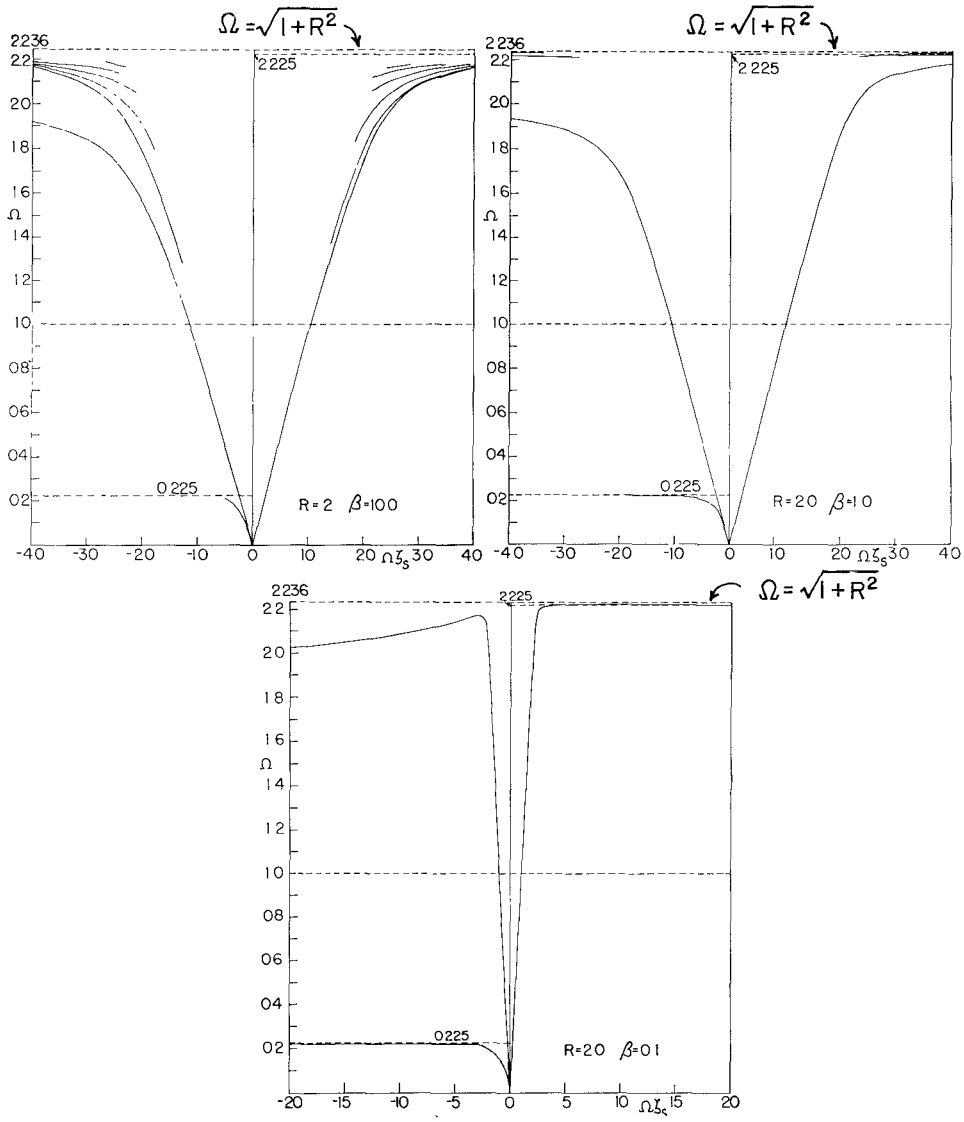

Fig. 5—Dispersion curves for the surface waves.

cutoff Ω_c becomes greater than Ω_{a1}, and the dispersion curve overshoots the asymptotic line. For extremely small sheath thickness such as $\beta = 10^{-3}$, the cutoff frequency Ω_c approaches $\Omega = \sqrt{1+R^2}$.

For the case $R = 0.5$, the two asymptotes corresponding to negative values of ζ_s, coincide. Hence, both the dispersion curves for $\beta = 10$ approach this common asymptote; also they have no low frequency cutoff or backward wave regions. As β is progressively reduced, the general behavior of the dispersion curve corresponding to the faster of the two waves, is the same as that of the dispersion curve corresponding to positive ζ_s. But the phase velocity of the slower of the two waves is progressively reduced as the sheath thickness is made smaller, with the result that the corresponding dispersion curves do not exhibit backward wave regions nor do they overshoot the asymptote. The dependence of the dispersion curves on the sheath thickness, as described above, is true even when R is not equal to 0.5 as can be inferred from Fig. 5.

The phase velocity of the surface waves is easily seen to be given by c_0/ζ_s where c_0 is the velocity of electromagnetic waves in free space. Since $\zeta_s \geq 1$, it follows that the surface wave is always a slow wave. The phase velocity of the Type 2 surface waves at extremely low frequencies reveals certain interesting features. With the help of (4b), (21) for very small Ω becomes

$$1 - \frac{R^2\zeta_s^2}{R^2+1} - \frac{R\zeta_s\sqrt{\zeta_s^2-1}}{\Omega(R^2+1)} = \frac{\sqrt{\zeta_s^2-1}}{\Omega\sqrt{R^2+1}}. \quad (27)$$

When the roots of (27) are obtained as a power series in Ω and only the leading terms are retained, the result is

$$\zeta_s = 1 \quad (28a)$$

$$\zeta_s = -1 \quad (28b)$$

$$\zeta_s = -\sqrt{1+R^2}/R \quad (28c)$$

It has been shown [10] that two unidirectional surface waves can exist along the interface between a semi-infinite free space and a semi-infinite gyrotropic dielec-

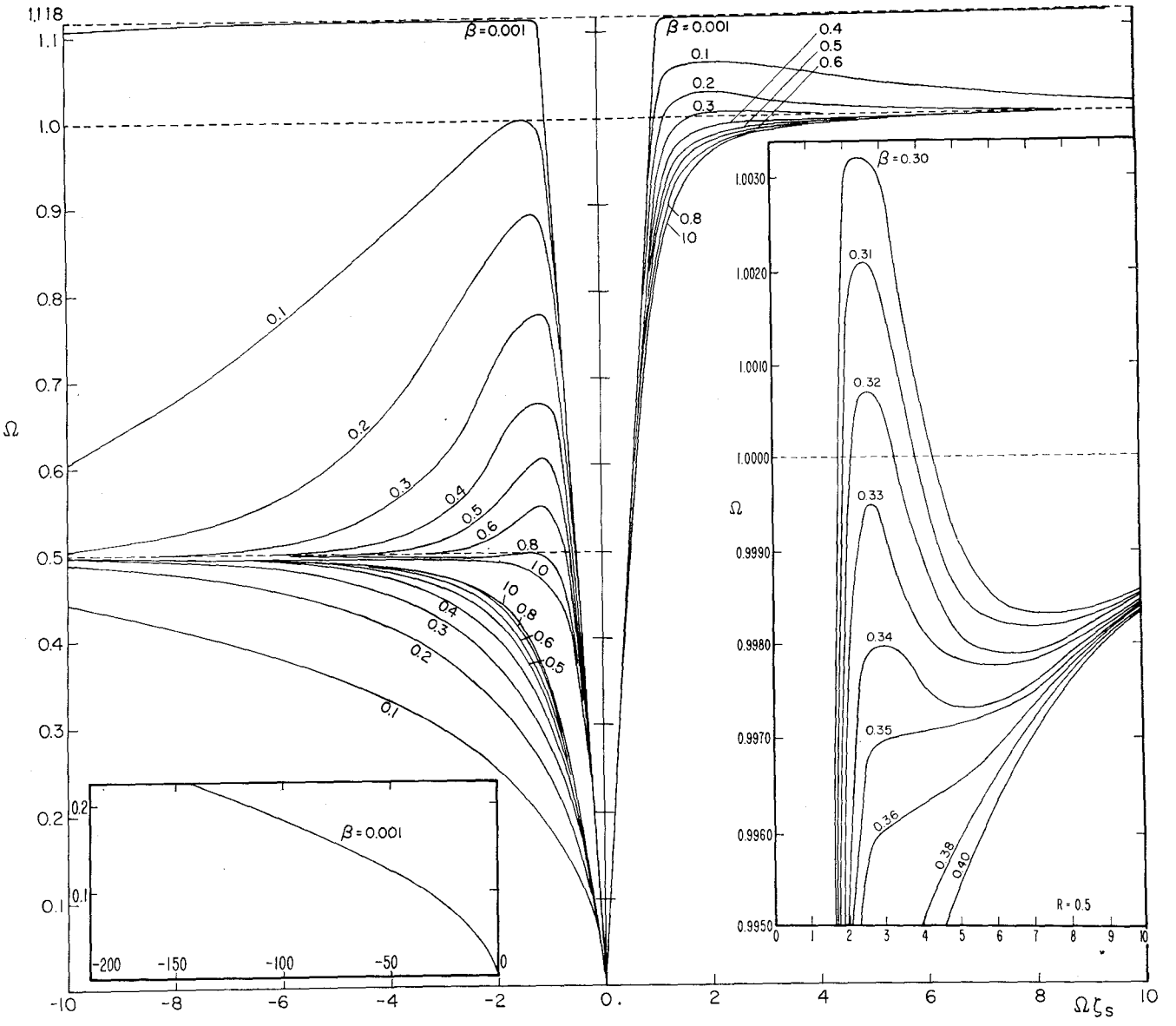

Fig. 6—Dispersion curves for type 2 surface waves as a function of sheath thickness.

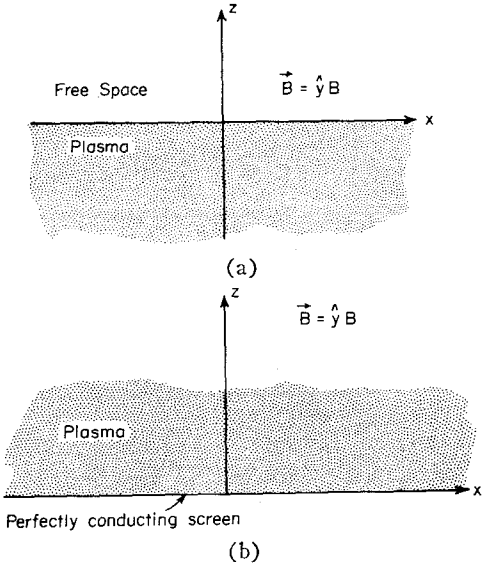

Fig. 7—(a) Plane interface between semi-infinite regions of free space and plasma. (b) Perfectly conducting screen covered with a semi-infinite region of plasma.

tric. The surface wave traveling in the positive (negative) x-direction [Fig. 7(a)] has a high frequency cutoff at $\Omega=\Omega_{a1}(\Omega_{a2})$. Both these surface waves at extremely low frequencies, travel with a phase velocity c_0. The exponential attenuation of the wave transverse to the interface in the plasma and in free space are, respectively, governed by the factors $\exp(-k_0\sqrt{|\epsilon/\epsilon_1|+\zeta_s^2})z$ and $\exp(-k_0\sqrt{\zeta_s^2-1})z$. Since as $\Omega\to 0$, $|\epsilon/\epsilon_1|\to\infty$, and $|\zeta_s|\to 1$, it follows that the surface wave is extremely rapidly attenuated in the plasma and practically unattenuated in free space. Therefore, the termination of the plasma by a perfectly conducting screen, parallel to the interface, should not materially affect these surface waves. These unidirectional surface waves may then be easily identified with the Type 2 surface waves whose dispersion curves have for their asymptotes $\Omega=\Omega_{a1}$ and $\Omega=\Omega_{a2}$ and whose phase velocities for $\Omega\to 0$ are given by (28a, b). These Type 2 surface waves may be considered to be essentially guided along the interface between free space and the plasma slab.

Also, it has been shown [9], [11], [12] that unidirectional surface waves traveling in the negative x-direction for $0<\Omega<R$ and in the positive x-direction for $\sqrt{1+R^2}<\Omega<\infty$, are supported by a perfectly conducting screen covered with anisotropic plasma [Fig. 7(b)]. It has been suggested [9] that these unidirectional surface waves become leaky waves when the plasma thickness is finite. While the surface waves in the frequency range $\sqrt{1+R^2}<\Omega<\infty$ change into complex waves [4] for a finite thickness of the plasma, the same is not true for the surface waves in the frequency range $0<\Omega<R$. The unidirectional surface wave on a perfectly conducting screen covered with plasma, has the spatial dependence of the form $\exp(-k_0\sqrt{\epsilon_1}\,x-(|\epsilon_2|/\sqrt{\epsilon_1})z)$. From (4b) it is obvious that for $\Omega\to 0$, the normalized wave number of this surface wave is $\sqrt{1+R^2}/R$ which is the same as given in (28c). Note that $|\epsilon_2|/\sqrt{\epsilon_1}\to\infty$ as $\Omega\to 0$. Therefore this unidirectional surface wave is extremely rapidly attenuated in the plasma and hence, should not be affected by terminating the plasma by free space at a finite distance from the perfectly conducting screen. Consequently, it is proper to conclude that the Type 2 surface wave, on the anisotropic slab belonging to the dispersion curve having for its asymptote $\Omega=\Omega_{a3}=R$, is essentially guided by the perfectly conducting screen.

V. Power in the Surface Waves

It is proposed to determine the surface and the space wave parts of the total field by evaluating the integrals (7a, b). The forward and the backward surface wave poles are conveniently distinguished by the additional subscripts f and b. The contours for the integrals (7a, b) are along the real axis in the ζ-plane as shown in Fig. 8. The surface wave poles are on the real axis, and the integration contour has to be suitably indented (see Fig. 8) in the vicinity of these poles, such that the radiation condition is satisfied. For $x>0$, the integrals may be evaluated by closing the contour in the upper half of the ζ-plane. The contribution to the integrals (7a, b) is the sum of the residue at the poles and a branch-cut integral. For sufficiently large $|x|$, the branch-cut contribution is negligible compared to that due to the pole. Hence, for large positive x, after some simplification, the following results are obtained:

$$1)\quad H_y^s(x,z)=\frac{-\omega\epsilon_0\epsilon E_{x0}}{\Delta'(k_s)}\Big[\epsilon_1\sqrt{k_s^2-k^2}\cosh(z-d)\sqrt{k_s^2-k^2}-\{\epsilon\sqrt{k_s^2-k_0^2}+\epsilon_2 k_s\}\sinh(z-d)\sqrt{k_s^2-k^2}\Big]e^{ik_sx}\quad(29a)$$

$$2)\quad H_y^s(x,z)=\frac{-\omega\epsilon_0\epsilon E_{x0}\epsilon_1\sqrt{k_s^2-k^2}}{\Delta'(k_s)}e^{ik_sx-\sqrt{k_s^2-k_0^2}(z-d)}\quad(29b)$$

where I and II refer, respectively, to the plasma and the vacuum regions and $\Delta'(k_s)$ equals $d/d\zeta\Delta(\zeta)$ evaluated at $\zeta=k_s$. The expressions (29a, b) are appropriate only to the Type 2 surface waves. It is not difficult to write the corresponding forms suitable for the Type 1 surface waves. Obviously, $H_y^s(x,z)$ given in (29a, b) represents surface waves propagating in the positive x-direction and exponentially attenuated in the z-direction in the vacuum region.

Let P_{s+}^{I} and P_{s+}^{II} be the power transported by the surface wave per unit length of the source in the positive x-direction in the plasma and the vacuum regions, respectively. Then, it can be shown that,

$$P_{s+}^{\mathrm{I}}=-\frac{1}{2}\,\mathrm{Re}\int_0^t E_z^s(x,z)H_y^{s*}(x,z)\,dz$$

$$P_{s+}^{\mathrm{II}}=-\frac{1}{2}\,\mathrm{Re}\int_t^\infty E_z^s(x,z)H_y^{s*}(x,z)\,dz.\quad(30)$$

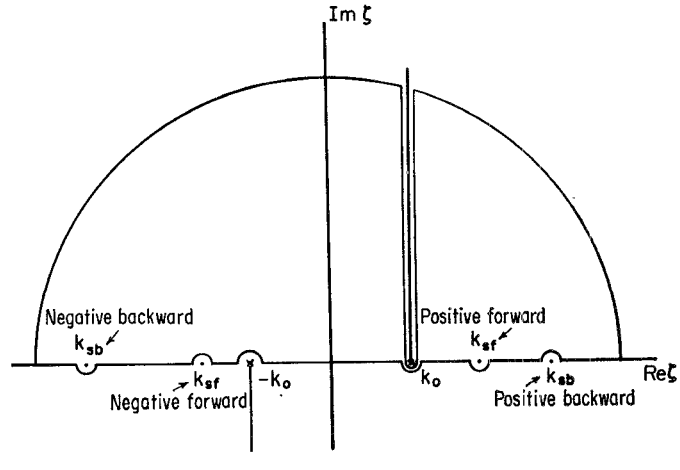

Fig. 8—Contour of integration in the ζ-plane.

On using (5) and (29) in (30) and simplifying the resulting expression with the help of (8) and (11), it follows that

$$P_{s+}^{\mathrm{I}} = \frac{1}{2}\omega\epsilon_0 E_{x0}^2 \frac{1}{\epsilon D^2}\left[A\beta + \frac{B}{2}\left\{1 - \cosh 2\beta\sqrt{\zeta_s^2 - \frac{\epsilon}{\epsilon_1}}\right\} + \frac{C}{2}\frac{\sinh 2\beta\sqrt{\zeta_s^2 - \frac{\epsilon}{\epsilon_1}}}{\sqrt{\zeta_s^2 - \frac{\epsilon}{\epsilon_1}}}\right] \tag{31a}$$

$$P_{s+}^{\mathrm{II}} = \frac{1}{2}\omega\epsilon_0 E_{x0}^2 \frac{\zeta_s\epsilon_1^2}{2D^2}\frac{\left(\zeta_s^2 - \frac{\epsilon}{\epsilon_1}\right)}{\sqrt{\zeta_s^2 - 1}} \tag{31b}$$

where,

$$A = \frac{\epsilon_1\zeta_s}{2}\left\{\epsilon_1^2\left(\zeta_s^2 - \frac{\epsilon}{\epsilon_1}\right) - (\epsilon\sqrt{\zeta_s^2 - 1} + \epsilon_2\zeta_s)^2\right\} \tag{32a}$$

$$B = -\epsilon_1^2\zeta_s(\epsilon\sqrt{\zeta_s^2 - 1} + \epsilon_2\zeta_s) + \frac{\epsilon_2}{2}\left\{\epsilon_1^2\left(\zeta_s^2 - \frac{\epsilon}{\epsilon_1}\right) + (\epsilon\sqrt{\zeta_s^2 - 1} + \epsilon_2\zeta_s)^2\right\} \tag{32b}$$

$$C = \frac{\epsilon_1\zeta_s}{2}\left\{\epsilon_1^2\left(\zeta_s^2 - \frac{\epsilon}{\epsilon_1}\right) + (\epsilon\sqrt{\zeta_s^2 - 1} + \epsilon_2\zeta_s)^2\right\} - \epsilon_1\epsilon_2\left(\zeta_s^2 - \frac{\epsilon}{\epsilon_1}\right)(\epsilon\sqrt{\zeta_s^2 - 1} + \epsilon_2\zeta_s) \tag{32c}$$

$$D = \zeta_s\left[-\epsilon_1\sqrt{\frac{\zeta_s^2 - 1}{\zeta_s^2 - \frac{\epsilon}{\epsilon_1}}} - \epsilon_1\sqrt{\frac{\zeta_s^2 - \frac{\epsilon}{\epsilon_1}}{\zeta_s^2 - 1}} + \frac{\epsilon_1\beta}{\sqrt{\zeta_s^2 - \frac{\epsilon}{\epsilon_1}}} + \frac{\beta\zeta_s^2}{\sqrt{\zeta_s^2 - \frac{\epsilon}{\epsilon_1}}} + \epsilon_2\beta\zeta_s\sqrt{\frac{\zeta_s^2 - 1}{\zeta_s^2 - \frac{\epsilon}{\epsilon_1}}}\right]$$
$$\cdot \cosh\beta\sqrt{\zeta_s^2 - \frac{\epsilon}{\epsilon_1}} + \left[-\epsilon_1\zeta_s\beta\sqrt{\zeta_s^2 - 1} - 2\zeta_s + \epsilon_2\sqrt{\zeta_s^2 - 1} + \frac{\epsilon_2\zeta_s^2}{\sqrt{\zeta_s^2 - 1}}\right]\sinh\beta\sqrt{\zeta_s^2 - \frac{\epsilon}{\epsilon_1}}\cdot \tag{32d}$$

The total power transported in the positive x-direction by the surface wave is given by

$$P_{s+} = P_{s+}^{\mathrm{I}} + P_{s+}^{\mathrm{II}}. \tag{33}$$

The power transported in the negative x-direction in the regions I and II and the total power transported in the negative x-direction, are denoted by P_{s-}^{I}, P_{s-}^{II}, and P_{s-}, respectively; the expressions for these may be evaluated in a similar fashion and are found to be the same as the corresponding quantities for the positive x-direction, with an added minus sign. For a positive forward and a negative backward surface wave pole, P_{s+} will be positive, showing that these poles contribute to power transport in the positive x-direction. Similarly, a negative forward and a positive backward surface wave pole will contribute to power transport in the negative x-direction.

In the rest of this paper, only normalized powers will be used, and these are obtained by the removal of the factor $\frac{1}{2}\omega\epsilon_0 E_{x0}^2$. With the help of (31), the normalized powers are evaluated as a function of sheath thickness for two sets of values for the parameters R and Ω, and the results are depicted in Figs. 9 and 10. For $R = 0.5$ and $\Omega = 0.5514$ and for the range of sheath thickness shown in Fig. 9, there is one positive forward, one negative forward, and one negative backward surface wave pole. Consequently, a forward wave and a backward wave contribute to power transport in the positive x-direction whereas the power transport in the negative x-direction is due only to a forward wave. It can be seen from Fig. 9, that the backward wave transports considerably more power in the positive x-direction than the simultaneously excited forward wave. For the situation shown in Fig. 9, it was found that no matter whether it is a backward wave or a forward wave, for a particular β, the slower wave transported more power than the faster. Since the backward wave happened to be the slowest, it carried more power.

For $R = 0.5$ and $\Omega = 0.9991$ (Fig. 10), there are no negative poles. For each sheath thickness β, there is one backward and two forward surface wave poles, and these are all positive. The power transport in the posi-

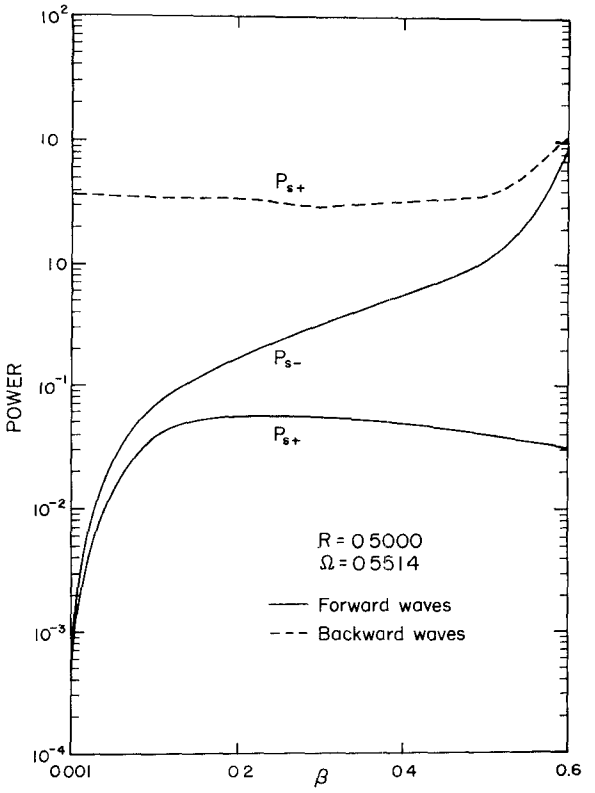

Fig. 9—Power in the surface waves as a function of β.

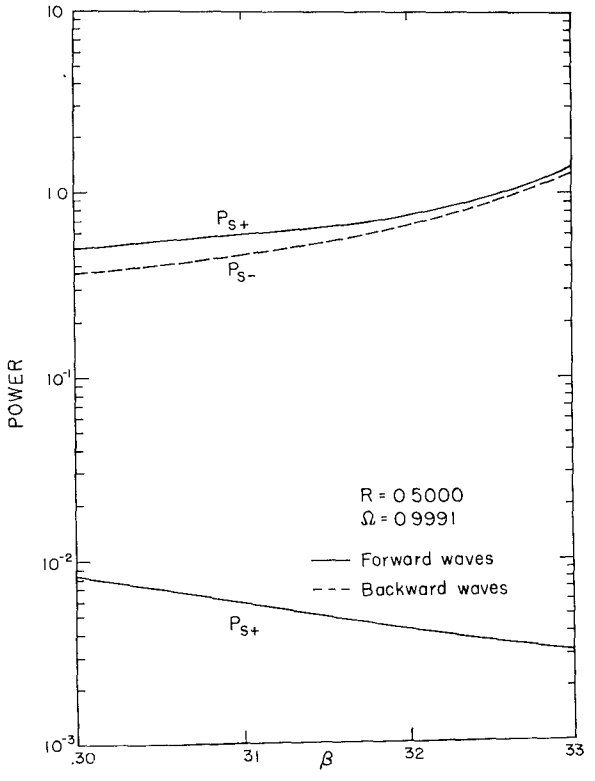

Fig. 10—Power in the surface waves as a function of β.

tive x-direction is contributed by two forward waves whereas, the power transport in the negative x-direction is due only to a backward wave. Also in this case, the faster wave transported more power than the slower wave. Since a backward wave is always accompanied by a faster forward wave, the power transported by the faster forward wave is higher than that of the slower backward wave. In the negative x-direction, only the backward surface wave exists, and this makes it possible for verification by a suitably designed experiment.

VI. Power in the Space Waves

The space wave part of the total field is obtained by performing a saddle-point evaluation of the integral (7b) with the following result for $k_0 0 \gg 1$;

$$H_y(\rho, \phi) = -\omega\epsilon\epsilon_1 E_{x0} e^{-ik_0 d \sin\phi} \cdot \frac{e^{i(k_0\rho - \pi/4)}}{\sqrt{2\pi k_0 \rho}} \frac{\epsilon k_0^2 \sin\phi \sqrt{\frac{\epsilon}{\epsilon_1} - \cos^2\phi}}{\Delta(k_0 \cos\phi)} \tag{34}$$

$$x = \rho\cos\phi \qquad z = \rho\sin\phi. \tag{35}$$

The outward power flow per unit area, per unit distance in the y direction at an angle ϕ, is obtained from (34) using (5b), (8) and (35) to be

$$S_\rho = \frac{1}{2} \operatorname{Re} \hat{\rho} \cdot \boldsymbol{E}(\rho, \phi) \times \boldsymbol{H}^*(\rho, \phi) = \frac{k_0}{2\omega\epsilon_0} \left| H_y(\rho, \phi) \right|^2 = \frac{1}{2} \omega\epsilon_0 E_{x0}^2 \frac{f(\phi)}{2\pi\rho} \tag{36}$$

where

$$f(\phi) = \epsilon_1^2 \sin^2\phi \left| \frac{\epsilon}{\epsilon_1} - \cos^2\phi \right| \cdot \left[\sin^2\phi \left\{ \epsilon_1 \sqrt{\frac{\epsilon}{\epsilon_1} - \cos^2\phi} \cos\beta \sqrt{\frac{\epsilon}{\epsilon_1} - \cos^2\phi} - \epsilon_2 \cos\phi \sin\beta \sqrt{\frac{\epsilon}{\epsilon_1} - \cos^2\phi} \right\}^2 + \left\{ \epsilon_1 - \cos^2\phi \right\}^2 \sin^2\beta \sqrt{\frac{\epsilon}{\epsilon_1} - \cos^2\phi} \right]^{-1}$$

$$\text{for } 0 \leq \phi \leq \pi. \tag{37}$$

In Fig. 11, the radiation pattern $f(\phi)$ given by (37), is plotted for the case $R = 2.0$ and $\Omega = 1.0$, for ten different values of the sheath thickness β. It is seen that there is always a broad maximum near the broadside direction, a null in the end-fire direction, and in between, sharply defined peaks whose number increase with the sheath thickness β.

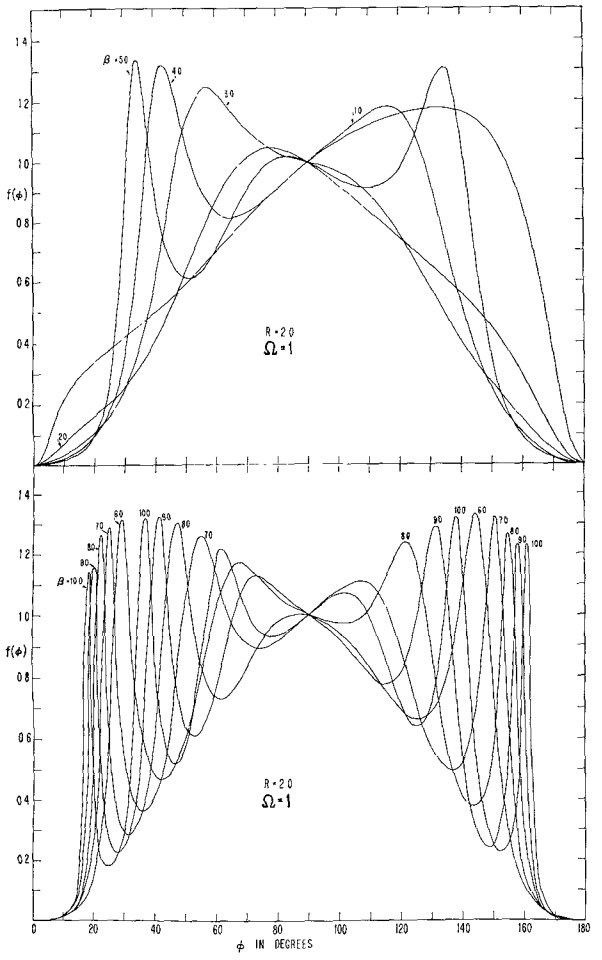

Fig. 11—Radiation pattern: $R=2.0$.

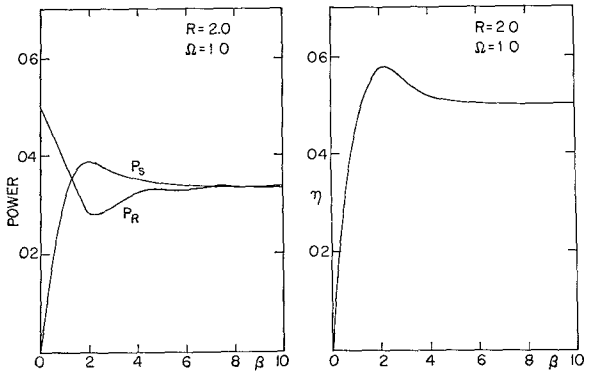

Fig. 12 (left)—Power in the surface wave (P_S) and in the radiated space wave (P_R) as a function of β.
Fig. 13 (right)—Efficiency of excitation of surface waves as a function of β.

The total power radiated in the space waves, after being normalized, as before is given by

$$P_R = \frac{1}{2\pi}\int_0^{\pi} f(\phi)d\phi. \tag{38}$$

The value of P_R for the case $R=2.0$ and $\Omega=1.0$ is plotted in Fig. 12 as a function of the sheath thickness β. As the sheath thickness β is increased, the total power in the space waves oscillates several times and that in the surface wave oscillates once, but eventually both approach a constant value.

For $R=2.0$, $\Omega=1.0$, and $1\leq\beta\leq10$, there is one positive and one negative forward surface wave pole. The normalized surface wave powers, P_{s-} and P_{s+} transported in the negative and the positive x-directions, and therefrom the total power in the surface wave $P_s=P_{s-}+P_{s+}$, are evaluated. The total power P_s carried by the surface waves is also plotted in Fig. 12, as a function of the sheath thickness β. It is seen that the surface wave power also approaches a constant value for large sheath thickness and, for the present example, this constant value is the same as that approached by the radiated power P_R.

The efficiency of excitation η of the surface wave is defined as

$$\eta = P_s/(P_s + P_R) \tag{39}$$

where P_s and P_R are the powers propagated in the form of the surface and space waves respectively. For $R=2.0$ and $\Omega=1.0$, the efficiency η is plotted in Fig. 13. Except for extremely small β, a considerable portion of the total power is seen to be propagated in the form of the surface waves. In the present example, η approaches 0.5 for very large β showing that the total power radiated by the source is equally divided between the space waves and the surface waves. Also there is a particular value of sheath thickness for which η is a maximum. The excitation efficiency η will be different for other values of the parameters Ω and R as it also is for a distributed source, which can be designed to put relatively more power in the surface waves and less into the space waves.

From Fig. 4 it is obvious that the negative surface wave pole belongs to the dispersion curve which has for its asymptote $\Omega=R$. With the help of the discussion in Section IV, it follows that the surface wave contributed by this pole is essentially guided by the perfectly conducting screen. The arguments leading to this deduction are still further strengthened by a comparison of the magnitudes of P_{s-}^{I} and P_{s-}^{II} which are the powers transported in the negative x-direction in the plasma and vacuum regions, respectively. Except for small sheath thickness such as $\beta=1.0$, it is found that P_{s-}^{II} is negligible compared to P_{s-}^{I}. For $\beta\geq2.0$, P_{s-}^{II} is less than one per cent of P_{s-}^{I} and for $\beta=10$, P_{s-}^{II} is less than 10^{-3} per cent of P_{s-}^{I}. These results may be interpreted to mean that this surface wave is essentially guided by the perfectly conducting screen. In the present example, it is found also that P_{s+} is considerably smaller than P_{s-} and for large sheath thickness, P_{s+} is negligible compared to P_{s-}. As the sheath thickness is increased without limit, the surface wave transporting power in the positive x-direction becomes progressively extinct and in the limit of semi-infinite plasma only the surface wave transporting power in the negative x-direction remains. This is exactly what is to be expected from the results of the previous investigation [11] which treated the excitation of surface waves on a perfectly conducting screen

covered with a semi-infinite layer of gyrotropic plasma.

In conclusion, it is pointed out, that a comprehensive treatment of the surface waves on a perfectly conducting screen covered with an anisotropic plasma sheath, is given for one simple orientation of the external magnetic field. The results of this paper are believed to provide an interesting extension to the results obtained by Tamir and Oliner [3] for the isotropic case.

ACKNOWLEDGMENT

The authors are grateful to Prof. R. W. P. King for help and encouragement with this research.

REFERENCES

[1] A. A. Oliner and T. Tamir, "Backward waves on isotropic slabs," *J. Appl. Phys.*, vol. 33, pp. 231–233; January, 1962.
[2] —— "The influence of complex waves on the radiation field of a slot-excited plasma layer," IRE TRANS. ON ANTENNAS AND PROPAGATION, vol. AP-10, pp. 55–65; January, 1962.
[3] ——, "The spectrum of electromagnetic waves guided by a plasma layer," PROC. IEEE, vol. 51, pp. 317–332; February, 1963.
[4] —— "Guided complex waves: Part I. Fields at an interface; Part II. Relation to radiation patterns," *Proc. IEE (London)* vol. 110, pp. 310–334; February, 1963.
[5] J. R. Wait, "The electromagnetic field of a dipole in the presence of a thin plasma sheet," *Appl. Sci. Res.*, Sect. B, vol. 8, pp. 397–417; 1961.
[6] ——, "Propagation of electromagnetic waves along a thin plasma sheet," *Can. J. Phys.*, vol. 38, pp. 1586–1594; December, 1960.
[7] R. Shore and G. Meltz, "Anisotropic plasma-covered magnetic line source," IRE TRANS. ON ANTENNAS AND PROPAGATION, vol. AP-10, pp. 78–82; January, 1962.
[8] H. Hodara and G. I. Cohn, "Radiation from a gyro-plasma coated magnetic line source," IRE TRANS., ON ANTENNAS AND PROPAGATION, vol. AP-10, pp. 581–593; September, 1962.
[9] A. Ishimaru, "The effect on the radiation from a plasma sheath of a unidirectional surface wave along a perfectly conducting plane," College of Engineering, University of Washington, Seattle, Wash., Tech. Rept. No. 64; April, 1962.
[10] S. R. Seshadri and A. Hessel, "Radiation from a source near a plane interface between an isotropic and a gyrotropic dielectric," Applied Research Laboratory, Sylvania Electronic Systems, Waltham, Mass., Research Rept. No. 339; May, 1963.
[11] S. R. Seshadri, "Excitation of surface waves on a perfectly conducting screen covered with anisotropic plasma", IRE TRANS. ON MICROWAVE THEORY AND TECHNIQUES, vol. MTT-10, pp. 573–578; November, 1962.
[12] ——, "Scattering of unidirectional surface waves," IEEE TRANS. ON MICROWAVE THEORY AND TECHNIQUES, vol. MTT-11, pp. 238–243; July, 1963.

Back-Scattering Measurements of a Slowly Moving Target

O. P. McDUFF, MEMBER, IEEE, H. MOTT, SENIOR MEMBER, IEEE, AND C. S. DURRETT, JR., MEMBER, IEEE

Summary—A basic problem in the measurement of back-scattering cross sections is the separation of the desired target-scattered signal from the undesired background reflections. An additional problem may be the separation from the target-scattered signal of signals directly coupled from the transmitter to the receiver. Historically, these have been overcome in several ways: 1) a reference signal has been used to cancel the undesired signals when measuring a fixed target, 2) a reference signal has been used to override the undesired signals when measuring a rapidly moving target, and 3) an average curve has been fitted to data taken with a target at several positions.

Two useful alternative techniques are described herein. A cancellation procedure performed while the target is slowly moving is shown to be effective in a much poorer environment than the static nulling procedure. The use of a reference signal to override the undesired signals is shown to be directly applicable to a slowly moving target procedure, thus simplifying the mechanical problems in measuring bulky targets. With a simple experimental setup, back-scattering cross sections 33 db below a square wavelength at 11 Gc can be measured at a range of 150 cm when transmitting 400 mw. These readings can be taken in an environment 20 to 30 db worse than that usually considered necessary for scattering measurements by the static null procedure.

Manuscript received October 14, 1963; revised May 4, 1964. This work was supported by the National Aeronautics and Space Administration under Contract NAS8-5011.

The authors are with the Electrical Engineering Department, University of Alabama, University, Ala.

INTRODUCTION

THE THEORETICAL determination of the back-scattering cross section of any except simple symmetrically shaped objects is exceedingly difficult because of mathematical complexities. Even with simple shapes, it is satisfying to check theory with experimental results. Thus a number of experimental procedures have been developed for measuring the back-scatter cross section of objects with complex shapes.[1–7]

[1] D. D. King, "Measurement and interpretation of antenna scattering," PROC. IRE, vol. 37, pp. 770–777; July, 1949.
[2] J. Sevick, "An Experimental Method of Measuring Back-Scattering Cross Sections of Coupled Antennas," Cruft Lab., Harvard Univ., Cambridge, Mass., Tech, Rept. No. 151; May, 1952.
[3] H. Scharfman and D. D. King, "Antenna-scattering measurements by modulation of the scatterer," PROC. IRE, vol. 42, pp. 854–858; May, 1954.
[4] R. W. P. King and T. T. Wu, "The Reflection of Electromagnetic Waves from Surfaces of Complex Shapes," Cruft Lab., Harvard Univ., Cambridge, Mass., Sci. Rept. No. 12; November, 1957.
[5] H. J. Schmitt, "Back-scattering measurements with a space-separation method," IRE TRANS. on ANTENNAS AND PROPAGATION, vol. AP-7, pp. 15–32; January, 1959.
[6] C. C. H. Tang, "Electromagnetic backscattering measurements by a time-separation method," IRE TRANS. ON MICROWAVE THEORY AND TECHNIQUES, vol. MTT-7, pp. 209–213; April, 1959.
[7] E. B. McMillan and H. J. Schmitt, "Doppler method for absorber testing," *Microwave J.*, vol. 3, pp. 64–68; November, 1960.